remote sensing

MDPI

Article

A Novel Ambiguity Parameter Estimation and Elimination Strategy for GNSS/INS Tightly Coupled Integration

Chun Ma [1], Qiuzhao Zhang [1,*], Xiaolin Meng [2], Nanshan Zheng [1] and Shuguo Pan [3]

1 Jiangsu Key Laboratory of Resources and Environmental Information Engineering, China University of Mining and Technology, Xuzhou 221116, China; machun310@cumt.edu.cn (C.M.); znshcumt@cumt.edu.cn (N.Z.)
2 Sino-UK Geospatial Engineering Centre, University of Nottingham, Nottingham NG7 2TU, UK; xiaolin.meng@nottingham.ac.uk
3 School of Instrument Science and Engineering, Southeast University, Nanjing 210096, China; psg@seu.edu.cn
* Correspondence: qiuzhao.zhang@cumt.edu.cn; Tel.: +86-137-7598-9554

Received: 31 August 2020; Accepted: 20 October 2020; Published: 26 October 2020

Abstract: The estimation of ambiguity in the global navigation satellite system/inertial navigation system (GNSS/INS) tightly coupled system is a key issue for GNSS/INS precise navigation positioning. Only when the ambiguity is solved correctly can the integrated navigation system obtain high-precision positioning results. Aiming at the problem of ambiguity parameter estimation in GNSS/INS tightly coupled system, a new strategy for ambiguity parameter estimation and elimination is proposed in this paper. Here, the ambiguity parameter is first added to the state equations of GNSS/INS in the estimation process. Then, the strategy of eliminating the parameter is used to improve efficiency. A residual test is carried out based on introducing the ambiguity parameter, thereby reducing or avoiding its influence on the filtering estimation process. Two groups of experiments were carried out and compared with GNSS positioning results. The results showed that, in the open sky observation environment, the positioning accuracy of the GNSS/INS tightly coupled method proposed in this paper was within 5 cm, and the ambiguity fixed rate was more than 97%, which is basically consistent. In a GNSS-denied environment, the positioning accuracy of the GNSS/INS tightly coupled method proposed in this paper was obviously better than that of GNSS, and the positioning accuracy in X, Y, and Z directions was improved by 82.46%, 78.87%, and 79.67%, respectively. The fixed rate of ambiguity increased from 73% to 78.57%. Therefore, in a GNSS-challenged environment, the novel strategy of the GNSS/INS tightly coupled system has higher ambiguity fixed rate and significantly improves positioning accuracy and continuity.

Keywords: GNSS/INS; integrated navigation; tightly coupled; ambiguity resolution

1. Introduction

Global navigation satellite system (GNSS) real-time kinematic (RTK) technology is a real-time dynamic positioning technology based on carrier phase observations. In the case of a correct solution of ambiguity, it can achieve centimeter-level positioning accuracy, especially in short baseline positioning under an open sky field [1]. In GNSS-harsh environments, the attenuation, occlusion, and interruption of GNSS signals always cause the RTK technology to suffer from poor geometry and a reduction in the number of visible satellites, making it difficult to guarantee its position accuracy and reliability [2].

To solve this problem, GNSS is often integrated with inertial navigation system (INS) [3–5]. When GNSS is not available, INS can provide instantaneous high-precision position information without interruption, attitude information, and redundant geometric information for combined positioning [6,7]. Therefore, GNSS/INS high-precision combined positioning technology has attracted more and more attention in recent years and is widely used in fields such as autonomous driving, precision agriculture, and smart cities [8–10].

As with GNSS precision positioning, ambiguity resolution is a key and complex issue in GNSS/INS high-precision integrated positioning, especially in the harsh environment of single-frequency users [11,12]. In recent years, many ambiguity resolution algorithms have been continuously proposed. Among them, the most commonly used method is the least-squares ambiguity decorrelation adjustment method proposed by Teunissen, referred to as LAMBDA [13], and it has been proven to have the highest success rate [14]. The algorithm performs integer transformation to reduce correlation on the ambiguity float solution, performs integer least-square search to obtain the ambiguity integer solution, and then obtains the original ambiguity integer solution through integer inverse transformation. According to the combination mode, it can be divided into loosely coupled and tightly coupled systems. In the loosely coupled process, GNSS and INS work independently, and they cannot improve positioning accuracy and availability without providing additional information for the ambiguity solving process. In the tightly coupled system, the aid of inertial information for accurate position prediction in the ambiguity solving process can not only improve the search efficiency and ambiguity fixed success rate but also effectively improve the overall performance of the system when the satellite observation conditions are poor.

In the GNSS/INS tightly coupled strategy, there are two different implementation methods for estimating ambiguity parameters [15]. They both estimate the float ambiguity through least-squares or the extended Kalman filter (EKF). Subsequently, using the information of the corresponding covariance matrix, the search process is performed by the LAMBDA algorithm. The first method is to use INS position information as virtual observations to assist independent resolution of ambiguity and achieve fixed ambiguity. It has been experimentally verified that the introduction of INS information can reduce the ambiguity search space, but it does not give a rigorous search space expression [16]. Chen et al. derived a theoretical formula for the integer solution of ambiguity under inertial assistance, but the formula is too complicated and difficult to be practical [17]. Lee et al. proposed a pseudolite (PL) and INS-assisted single-frequency global positioning system (GPS) ambiguity resolution method for GPS/PL/INS integrated system, which can quickly and reliably solve ambiguity [18]. Gan et al. proposed a direct INS-assisted GPS ambiguity solution based on linear combined observations taking into account ionospheric error to achieve single epoch rounding and fixed ambiguity [19]. Han et al. proposed a single-frequency GPS/BeiDou navigation satellite system (BDS)/INS ambiguity fixed robust model by introducing a robust estimation function [20]. Subsequently, a new INS-assisted single-frequency GPS/BDS partial ambiguity resolution method was studied, and single-frequency GPS/BDS/INS integrated positioning was realized [21]. Li et al. proposed an anti-outlier ambiguity resolution and Kalman filter strategy based on the innovation of the outliers or poor-quality observations for a GPS/BDS/GLONASS/INS integrated positioning model, which can obtain high-precision positioning solutions [22]. Li et al. proposed an INS measurement method to aid integer ambiguity search in the position domain and correct the positioning status through carrier phase measurement, which can provide continuous and accurate positioning results under harsh GNSS signal conditions [23]. To improve positioning accuracy and ambiguity fixed rate in a GNSS-denied environment, other sensors, such as camera, odometer, and lidar, are used to assist the GNSS/INS tightly coupled system [24–26]. The abovementioned methods have a simple structure, high degree of modularity, and good independence. However, they require two filters to complete, and the calculation efficiency needs to be improved. Another issue is that the right moment of INS-aided GNSS filtering is difficult to determine.

The second method is to add the ambiguity parameter into the state equation of a GNSS/INS tightly coupled system and estimate and verify the ambiguity in the same filter. This method is mostly used in the precise point positioning (PPP)/INS tightly coupled system. The INS information is used to assist in PPP ambiguity resolution, which can effectively improve the speed of re-fixing the ambiguity after losing lock, but the initialization time is still long [27–30]. To improve the reliability of the RTK algorithm, Dorn et al. introduced single-difference ambiguity into the state equation to achieve high-precision positioning results, but it also introduced receiver clock bias and clock drift [31]. In the RTK/INS tightly coupled system, this method has been rarely studied, mainly due to the large number of state vectors when ambiguity parameters are introduced. In addition, it may lead to longer solution time and poor real-time performance of the system, especially in harsh environments. If there is a deviation in the ambiguity estimation of a satellite, this deviation estimation will affect the entire filtering process until the corresponding satellite is unavailable.

Therefore, to obtain positioning results with higher precision under a GNSS-challenged environment, ambiguity parameter estimation in the GNSS/INS tightly coupled system is very important. This paper proposes a new ambiguity parameter estimation and elimination strategy based on the state equation of GNSS/INS tightly coupled integration. Firstly, the double-difference ambiguity parameters are introduced into the filtering state equation for estimation. To better estimate the ambiguity parameters, a single-frequency and wide-lane combination strategy is adopted to improve the fixed success rate of ambiguity. Secondly, a strategy of eliminating parameters is used to reduce the amount of calculation required if the ambiguity is fixed correctly and there is no cycle slip, and the ambiguity is treated as a known amount. Finally, for a satellite, the deviation of ambiguity estimation will affect the whole filtering process. On this basis, a residual checking algorithm is used to avoid affecting the calculation of the next epoch or even the whole filtering process.

The rest of this paper is organized as follows. Section 2 describes the traditional GNSS/INS tightly coupled model, including the INS dynamic model and measurement model. In Section 3, a novel GNSS/INS tightly coupled algorithm is proposed to estimate and eliminate integer ambiguity parameters. In Section 4, the experimental results are described and compared with the results of GNSS only in different observation environments. The experimental results and performance of the algorithm are discussed in Section 5. Section 6 summarizes the conclusion of this paper and future research direction.

2. GNSS/INS Tightly Coupled Integration Model

In GNSS/INS tightly coupled navigation systems, the EKF is often used for system fusion. The EKF directly fuses the GNSS and inertial measurement unit (IMU) data to obtain optimal estimates of the integrated system state. To show the tightly coupled integration algorithm, the INS dynamic model and the measurement model will be introduced in this section.

2.1. INS Dynamic Model

For GNSS/INS integration, the system model generally consists of the INS dynamic model and sensor error. In this research, the IN dynamic model can be described as the following phi-angle error equations [32]:

$$\delta\dot{\boldsymbol{r}}^n = -\boldsymbol{\omega}_{en}^n \times \delta r^n + \delta\boldsymbol{\theta} \times \boldsymbol{v}^n + \delta\boldsymbol{v}^n \tag{1}$$

$$\delta\dot{\boldsymbol{v}}^n = C_b^n \delta\boldsymbol{f}^b + C_b^n \boldsymbol{f}^b \times \boldsymbol{\phi} - (2\boldsymbol{\omega}_{ie}^n + \boldsymbol{\omega}_{en}^n) \times \delta\boldsymbol{v}^n + \boldsymbol{v}^n \times (2\delta\boldsymbol{\omega}_{ie}^n + \delta\boldsymbol{\omega}_{en}^n) + \delta\boldsymbol{g}^n \tag{2}$$

$$\dot{\boldsymbol{\phi}} = -\boldsymbol{\omega}_{in}^n \times \boldsymbol{\phi} + \delta\boldsymbol{\omega}_{in}^n - C_b^n \delta\boldsymbol{\omega}_{ib}^b \tag{3}$$

where all parameters are with respect to the navigation frame. The symbols are defined as follows: $\delta\boldsymbol{\theta} = \begin{bmatrix} \delta r_E/(R_n+h) & -\delta r_N/(R_m+h) & -\delta r_E \tan\varphi/(R_n+h) \end{bmatrix}^T$, which is a rotation vector describing the misalignment of the computed frame with respect to the true navigation frame; R_m and R_n are the radiuses of curvature in the meridian and the prime vertical, respectively; h is the height; φ is the local geodetic latitude; $\delta\boldsymbol{r}$, $\delta\boldsymbol{v}$, and $\boldsymbol{\phi}$ are the position, velocity, and attitude error vectors, respectively; C_b^n represents the rotation matrix from the body frame (b) to the navigation frame (n); $\boldsymbol{\omega}_{en}^n$, $\boldsymbol{\omega}_{ie}^n$, and $\boldsymbol{\omega}_{in}^n$ represent the angle rate of the navigation frame relative to the Earth frame (e), the Earth frame relative to the inertial frame (i), and the navigation frame relative to the inertial frame, respectively, and $\delta\boldsymbol{\omega}_{en}^n$,

$\delta\boldsymbol{\omega}_{ie}^{n}$, and $\delta\boldsymbol{\omega}_{in}^{n}$ are the corresponding angular rate errors; $\boldsymbol{f}^{b}$ is the specific force on the body frame; $\delta\boldsymbol{g}^{n}$ is the normal local gravity error; and $\delta\boldsymbol{f}^{b}$ and $\delta\boldsymbol{\omega}_{ib}^{b}$ represent the sensor errors of the accelerometers and gyroscopes, respectively.

In inertial navigation, the sensor error is the most influential error source, including the error of the gyroscopes and the error of the accelerometers. The error equation of the inertial sensor is given as follows.

$$\delta\boldsymbol{\omega}_{ib}^{b} = \boldsymbol{s}_g \cdot \boldsymbol{\omega}_{ib}^{b} + \boldsymbol{b}_g + \boldsymbol{w}_g \tag{4}$$

$$\delta\boldsymbol{f}^{b} = \boldsymbol{s}_a \cdot \boldsymbol{f}^{b} + \boldsymbol{b}_a + \boldsymbol{w}_a \tag{5}$$

where $\boldsymbol{s}_g$, $\boldsymbol{b}_g$, $\boldsymbol{s}_a$ and $\boldsymbol{b}_a$ are the scale factors and bias errors of gyroscopes and accelerometers on each axis, respectively; $\boldsymbol{w}_g$ and $\boldsymbol{w}_a$ are white noise errors.

Therefore, the discrete form of the system state equation can be expressed as follows [33]:

$$\delta\boldsymbol{x}_{k+1} = \boldsymbol{\Phi}_{k+1,k}\delta\boldsymbol{x}_k + \boldsymbol{w}_k \tag{6}$$

where $\boldsymbol{\Phi}_{k+1,k}$ represents the system state transition matrix from epoch k to $k+1$, and ω_k represents the system process noise of epoch k; $\delta\boldsymbol{x} = \begin{bmatrix} \delta\boldsymbol{r} & \delta\boldsymbol{v} & \boldsymbol{\phi} & \boldsymbol{b}_g & \boldsymbol{b}_a \end{bmatrix}^T$ is the state vector of the system equation.

2.2. Measurement Model

In the GNSS/INS tightly coupled Kalman filtering model, the difference between the GNSS double-difference carrier phase observations and the "pseudophase" observations obtained by the double-difference geometric distance calculated by the INS is used as the innovation of the Kalman filtering.

The GNSS double-difference observation model under a short baseline can be expressed as follows:

$$\begin{cases} \lambda\nabla\Delta\varphi_{rb}^{jk} = \nabla\Delta r_{rb}^{jk} + \lambda\nabla\Delta N_{rb}^{jk} + e_{\nabla\Delta\Phi} \\ \nabla\Delta p_{rb}^{jk} = \nabla\Delta r_{rb}^{jk} + e_{\nabla\Delta p} \end{cases} \tag{7}$$

where the subscripts b and r are the base station and the rover station, respectively, and the combination represents the difference between the stations; the superscripts j and k are the observation satellites, j represents the reference satellite, and the combination represents the difference between the stars; and $\nabla\Delta r_{rb}^{jk}$ can be based on the known calculated amount.

The double-difference geometric distance calculated by the INS, that is, the double-difference geometric distance between the position of the carrier where the INS is located and the position of the reference station and the observation satellite, respectively, can be expressed as follows:

$$\begin{aligned} &\nabla\Delta\rho_{Ib}^{jk} = \Delta\rho_{Ib}^{j} - \Delta\rho_{Ib}^{k} \\ &= (e_{j1} - e_{k1})\delta x + (e_{j2} - e_{k2})\delta y + (e_{j3} - e_{k3})\delta z + \nabla\Delta r_{Ib}^{jk} \end{aligned} \tag{8}$$

where $\nabla\Delta r_{Ib}^{jk}$ can be calculated from the known quantity.

The difference between Formulas (7) and (8) can be used to obtain the innovation in tightly coupled Kalman filtering, which can be expressed as follows:

$$\begin{aligned} &\delta z_{\varphi} = \nabla\Delta\rho_{Ib}^{jk} - \lambda\nabla\Delta\varphi_{rb}^{jk} \\ &= (e_{j1} - e_{k1})\delta x + (e_{j2} - e_{k2})\delta y + (e_{j3} - e_{k3})\delta z - \lambda\nabla\Delta N^{jk} \end{aligned} \tag{9}$$

$$\begin{aligned} &\delta z_{p} = \nabla\Delta\rho_{Ib}^{jk} - \nabla\Delta\rho_{rb}^{jk} \\ &= (e_{j1} - e_{k1})\delta x + (e_{j2} - e_{k2})\delta y + (e_{j3} - e_{k3})\delta z \end{aligned} \tag{10}$$

The measurement equations for the tightly coupled system are

$$\delta \boldsymbol{z} = \boldsymbol{H}\delta \boldsymbol{x} + \boldsymbol{v} \tag{11}$$

where

$$\delta \boldsymbol{z} = \begin{bmatrix} \delta \boldsymbol{z}_{\varphi}^{T} & \delta \boldsymbol{z}_{p}^{T} \end{bmatrix}^{T} \tag{12}$$

$$\boldsymbol{H} = \begin{bmatrix} D \cdot C & 0_{n\times 3} & 0_{n\times 3} & 0_{n\times 6} & -\lambda I_n \\ D \cdot C & 0_{n\times 3} & 0_{n\times 3} & 0_{n\times 6} & 0_{n\times n} \end{bmatrix} \tag{13}$$

where D is the design coefficient of the position error vector; C is the error conversion matrix of space rectangular coordinate system and the geodetic coordinate system; v is the observation noise; n is the number of double differences; and $n = 1, 2, \cdots, m$. Theoretically, the error compensation term of the lever arm from the IMU to the antenna phase center should be expressed.

3. A Novel Ambiguity Parameter Estimation and Elimination Strategy

For INS parameter estimation, the state vector generally includes INS navigation parameter errors and inertial sensor bias errors. For GNSS, if the ambiguity parameter is unknown, it needs to be estimated to obtain the correct positioning result. In this paper, GNSS double-difference observations are mainly used for short baseline positioning, and only the double-difference ambiguity is estimated. Therefore, the double-difference ambiguity parameter should be estimated with other INS error parameters in the state equation of the tightly coupled system. Besides, if there is no cycle slip or signal loss of lock in the GNSS, the ambiguity will remain unchanged, which can be set as a constant value.

Assuming that there are $m + 1$ satellites, there are $15 + m$ state vectors for the GNSS/INS tightly coupled model. Excluding 15 INS state parameters, it also includes m double-difference ambiguity error parameters. Therefore, the error state vector of the tightly coupled model can be expressed as follows:

$$\delta \boldsymbol{x} = \begin{bmatrix} \delta \boldsymbol{r} & \delta \boldsymbol{v} & \boldsymbol{\phi} & \boldsymbol{b}_g & \boldsymbol{b}_a & \boldsymbol{N} \end{bmatrix}^{T} \tag{14}$$

where N represents m parameters of double-difference ambiguity, which can be expressed as follows:

$$\boldsymbol{N} = \begin{bmatrix} \nabla\Delta N_1 & \nabla\Delta N_2 & \cdots & \nabla\Delta N_m \end{bmatrix}^{T} \tag{15}$$

In fact, this method is similar to the idea of GNSS carrier measurement, which is to add the ambiguity parameter as an unknown parameter to the filter state estimation, construct an augmented matrix, and estimate and fix the ambiguity parameter in the filter [34]. However, different from the position, velocity, and ambiguity parameters in the GNSS state equation, the GNSS/INS state equation mainly consists of INS navigation error parameters and sensor error parameters. If the ambiguity parameter is added again, the calculation will be too heavy and error-prone, and it will be a catastrophic challenge for applications with high real-time requirements. Therefore, this is also the main reason the author wants to solve the problem.

In a GNSS-challenged environment, the ambiguity fixed success rate of single-frequency observations will decrease, resulting in poor positioning results. To improve the ambiguity fixed rate, wide-lane combination observations are used because the wavelength of the wide-lane combination is about 0.86 m, making the ambiguity easier to solve. Taking the GNSS carrier phase as an example, the double-difference observation equation can be expressed as follows:

$$z_k = \begin{bmatrix} \nabla\Delta\Phi_1 & \nabla\Delta\Phi_{WL} \end{bmatrix} \tag{16}$$

The coefficient matrix of the observation equation can be expressed as follows:

$$H_k = \begin{bmatrix} \frac{\partial\nabla\Delta\varphi_1}{\partial x} & \frac{\partial\nabla\Delta\varphi_1}{\partial y} & \frac{\partial\nabla\Delta\varphi_1}{\partial z} & 0 & 0 & 0 & 1 & 0 \\ \frac{\partial\nabla\Delta\varphi_{WL}}{\partial x} & \frac{\partial\nabla\Delta\varphi_{WL}}{\partial y} & \frac{\partial\nabla\Delta\varphi_{WL}}{\partial z} & 0 & 0 & 0 & 0 & 1 \end{bmatrix} \tag{17}$$

The observations of the combination of L1 and wide lanes are related because the observations of the combination of wide lanes are formed by the observations of L1. Given that the combined observations of the wide lane are formed by the observations of L1 and L2, it can be expressed as follows:

$$\begin{bmatrix} 1 & 0 \\ 1 & -1 \end{bmatrix} \begin{bmatrix} \varphi_1 \\ \varphi_2 \end{bmatrix} = \begin{bmatrix} \varphi_1 \\ \varphi_{WL} \end{bmatrix} \tag{18}$$

At this time, the combined measurement noise of L1 and wide lane can be expressed as follows:

$$\begin{bmatrix} 1 & 0 \\ 1 & -1 \end{bmatrix} \begin{bmatrix} \sigma_{L1} & 0 \\ 0 & \sigma_{L2} \end{bmatrix} \begin{bmatrix} 1 & 1 \\ 0 & -1 \end{bmatrix} = \begin{bmatrix} \sigma_{L1} & \sigma_{L1} \\ \sigma_{L1} & \sigma_{L1+L2} \end{bmatrix} \tag{19}$$

For the issue of too many parameters in the state vector, we can eliminate the fixed ambiguity parameters from the state vector if there is no cycle slip. For the ambiguity parameter in the tightly coupled system, the float ambiguity is obtained after extended Kalman filter estimation, which is then fixed by the LAMBDA algorithm and fed back to GNSS. If the ambiguity can be fixed correctly and no cycle slip occurs, it can be treated as a known quantity. At this time, the ambiguity parameter is eliminated from the state vector, and it is unnecessary to estimate it, which not only reduces the complexity of the Kalman filter but also greatly reduces the calculation workload. On the contrary, if the ambiguity is not fixed correctly, the updated state and covariance matrices of the Kalman filter need to be substituted into the estimation of the next epoch. At the same time, the observation value of the double-difference carrier formed by GNSS will also contain a high-precision float solution, which will greatly increase the fixed ambiguity.

With the above strategy, ambiguity parameter estimation in the GNSS/INS tightly coupled system can be realized. However, during the filtering process, if an ambiguity estimation is biased, it may affect the entire filtering process until the corresponding satellite is unavailable. At this time, the filtering process needs to be checked before or after each estimation to avoid the impact of this situation. The method based on innovation test is often used to deal with the impact of outlier problems, such as faulty satellites, strong multipath measurements, or undetected cycle slips on the filtering process. However, one problem with the innovation test is that the combination of measured values (which may be very accurate, such as carrier phase) and states (which may be very inaccurate because they are model-based) is not necessarily very accurate. Therefore, a residual test method is proposed in this paper. The residual test method is similar to the innovation test except that the residual is defined as follows:

$$\boldsymbol{v}_k^{(+)} = \boldsymbol{z}_k - \boldsymbol{H}_k \boldsymbol{x}_k^{(+)} \tag{20}$$

The covariance can be expressed as follows:

$$\boldsymbol{C}_{v_k^{(+)}} = \boldsymbol{H}_k \boldsymbol{P}_k^{(+)} \boldsymbol{H}_k^T + \boldsymbol{R}_k \tag{21}$$

The test statistic can be used to test the outlier problem generated during the filtering process, which is defined as follows:

$$t_{k_i} = \frac{\boldsymbol{m}_{k_i}^T \boldsymbol{C}_{v_k^{(+)}}^{-1} \boldsymbol{v}_k^{(+)}}{\sqrt{(C_{v_k^{(+)}}^{-1})i,i}} \tag{22}$$

where $\boldsymbol{m}_{k_i} = \begin{bmatrix} 0 & \cdots & 0 & 1 & 0 & \cdots & 0 \end{bmatrix}$ the ith position is 1.

The test statistic is used to test the null hypothesis that no outliers occur, defined as follows:

$$t_k|H_0 \sim N(0,1) \tag{23}$$

If $|t_k| \geq n_{(1-\alpha/2)}$, the null hypothesis is rejected. Assuming a Gaussian normal distribution, where $n_{(1-\alpha/2)}$ is a point on the axis and only $(1-\alpha/2)\%$ exceeds this point, if the threshold is defined as 3 standard deviations, the area under the curve is 0.997, which is approximately equal to the threshold of 3 standard deviations. However, in actual testing, it was found that when using the residual test, this number is quite strict because it will also be affected by measurements such as multipath. If the value used is 5, it is closer to 5–6 standard deviations.

It is worth noting that the outlier detection method based on a test has been studied by scholars for a long time. Among them, the more classic method is the detection, identification, and adaptation (DIA) method proposed by Teunissen et al. [35,36]. In DIA, the detection process aims to determine whether there is a certain deviation or outlier through the overall test; the identification process is used to determine which channel to measure or process vector and in which period the deviation or outlier occurs. In the adaptation process, the detected deviation and outlier will be corrected or discarded. The theoretical derivation of this method is relatively rigorous, and multiple epochs can be involved in the test. However, the process is more complicated, and there are also some problems, such as how to choose an appropriate alternative hypothesis. Although the residual test method proposed in this paper is only a single epoch test, it has a simple structure and is easy to use, although it needs further improvement.

Figure 1 shows the principle of GNSS/INS tightly coupled ambiguity resolution.

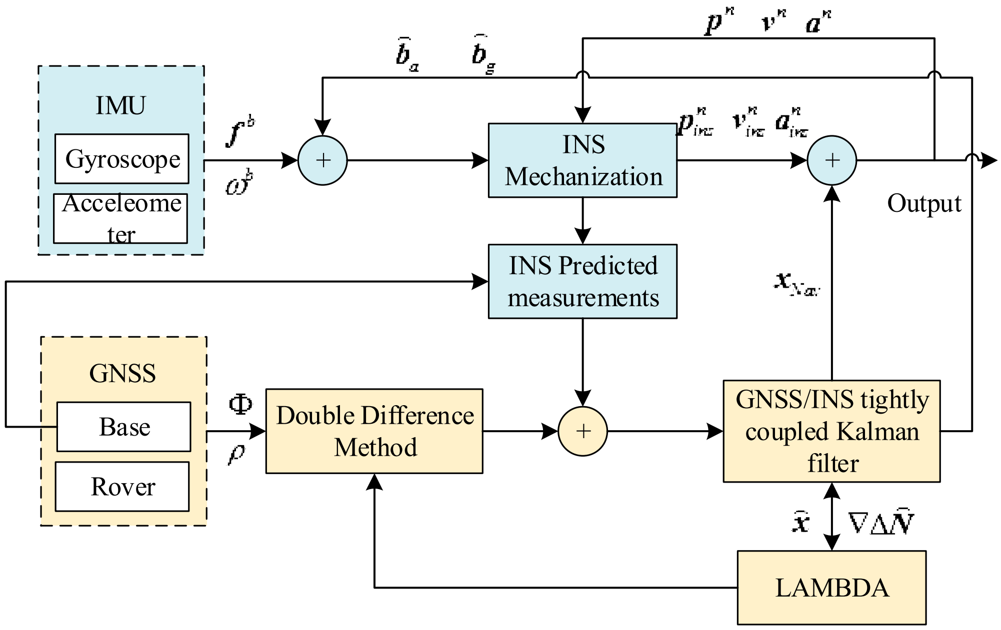

Figure 1. The principle of global navigation satellite system/inertial navigation system (GNSS/INS) tightly coupled ambiguity resolution.

4. Results

4.1. Open Sky Environment

The experimental data was collected on the roof of Nottingham Geospatial Building at the University of Nottingham, United Kingdom. In the experiment, the GNSS data of the reference station and rover station with 1 Hz were collected by a Leica dual-frequency receiver; the reference station was located on the roof of the building, and its coordinates were expressed in geodetic coordinates

(52.9519518690°, −1.184040010°, 96.680 m). The IMU raw data was collected using Honeywell's HG1700AG58, and the data sampling rate was 100 Hz. The specific technical parameters are shown in Table 1. The data collection time was about 24 min, and the maximum baseline length was about 50 m. In the experiment, dual-frequency data of the GPS was used for analysis, and the GPS/INS dual-frequency carrier tightly coupled smoothed result solved by the commercial software IE8.8 was used as a reference value.

Table 1. The technical parameters of HG1700AG58.

IMU	Bias	Random Walk	Scale Factor
Gyroscopes	1.0 deg/h	0.125 deg/sqrt(h)	150 ppm
Accelerometers	1.0 mg	-	300 ppm

Figure 2 shows the number of visible satellites and the position dilution of precision (PDOP) value of the rover during the experiment. It can be seen that the number of satellites was more than 7, and the overall observation environment was good. The PDOP value of the rover reflects the relationship with the number of visible satellites. The more visible satellites there are, the smaller is the PDOP value with better geometry. Figure 3 shows the velocity of the vehicle during the experiment. As the height was unchanged in the experiment on the roof, the velocity in the vertical direction was zero. However, when the vehicle started to move, the number of satellites began to decrease, and with each turn outside, the number of satellites was prone to change and changed frequently by the end of the experiment.

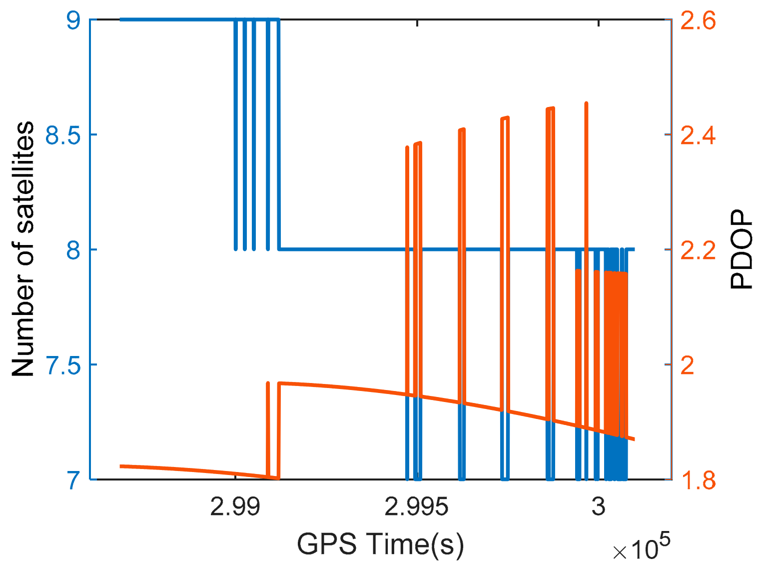

Figure 2. The number of visible satellites and the position dilution of precision (PDOP).

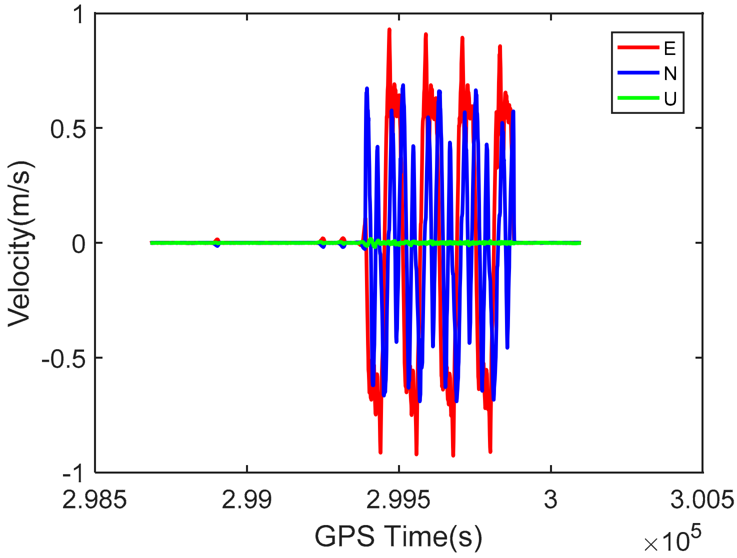

Figure 3. The velocity of the reference trajectory.

Figures 4 and 5 show the trajectory and height of the GPS solution and the tightly coupled solution with the reference value, respectively. As can be seen, the tightly coupled system performed better than the GPS results, and the GPS height error was greater. Both were relatively large in the initial stage, and the ambiguity was not yet fixed. Figure 6 shows the ambiguity status of the GPS and the tightly coupled system. Compared with the GPS fixed rate, the ambiguity fixed rate was slightly better at 97.81% and 99.58%, respectively.

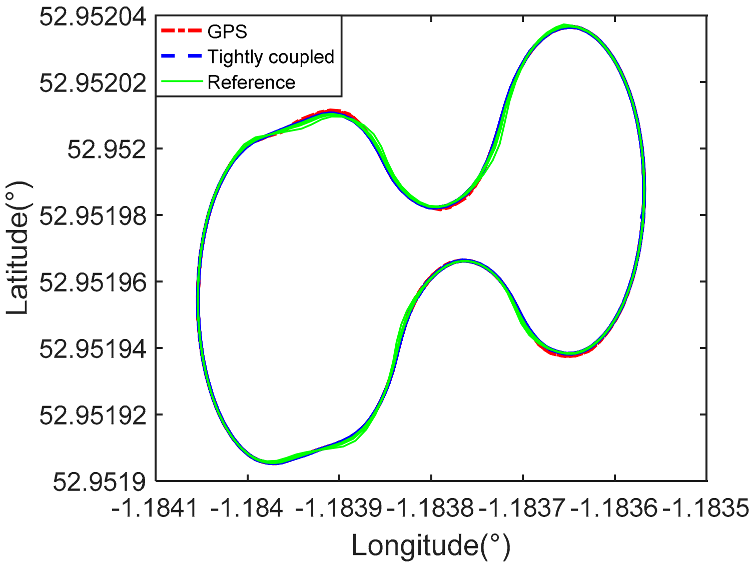

Figure 4. The trajectories of the three results.

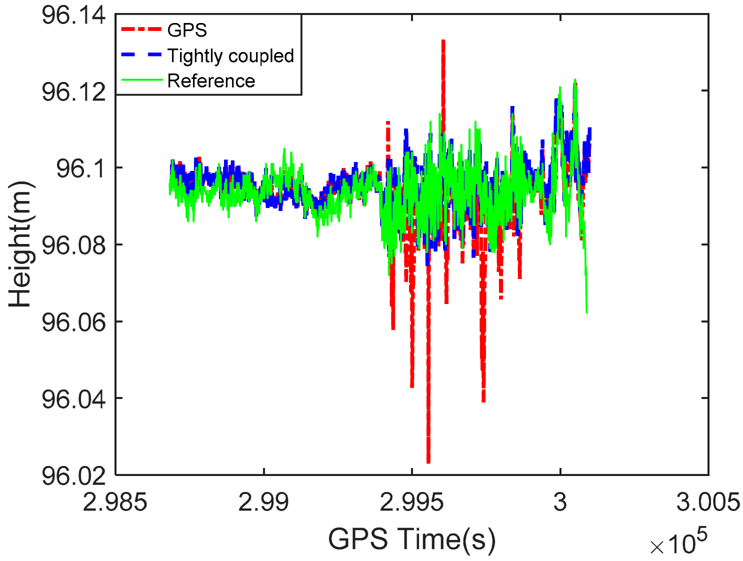

Figure 5. The height of the three results.

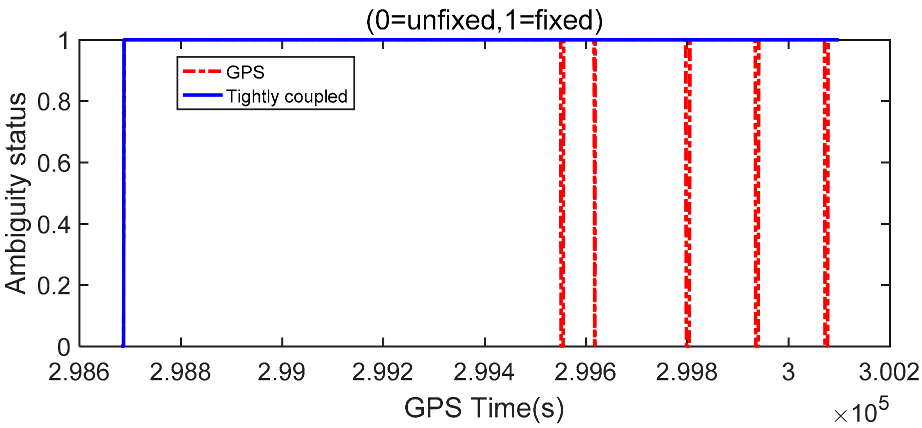

Figure 6. The ambiguity status of global positioning system (GPS) and the tightly coupled system.

Figures 7 and 8 show the position errors of GPS and the tightly coupled system with fixed initial ambiguity, respectively. For quantitative analysis, Table 2 gives the statistical results of the position error of GPS and the GPS/INS tightly coupled system. From Table 2, it can be seen that the positioning accuracy of GPS and the tightly coupled system in the three directions of X, Y, and Z were all within 5 cm. The positioning accuracy of the tightly coupled system was slightly higher.

Table 2. The statistical results of position errors of GPS and the tightly coupled system.

		Maximum (m)	Minimum (m)	RMS (m)
GPS	X	0.204	−0.268	0.045
	Y	0.179	−0.238	0.038
	Z	0.157	−0.116	0.022
Tightly coupled system	X	0.207	−0.273	0.044
	Y	0.161	−0.241	0.034
	Z	0.137	−0.122	0.017

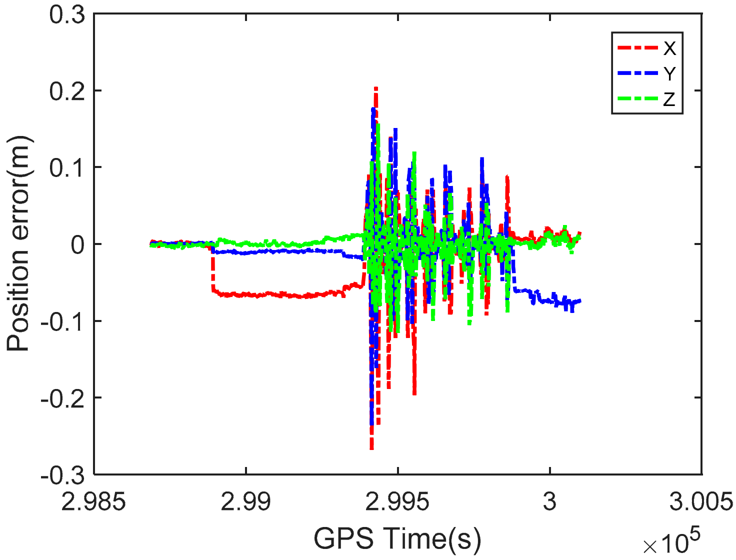

Figure 7. The position error of GPS.

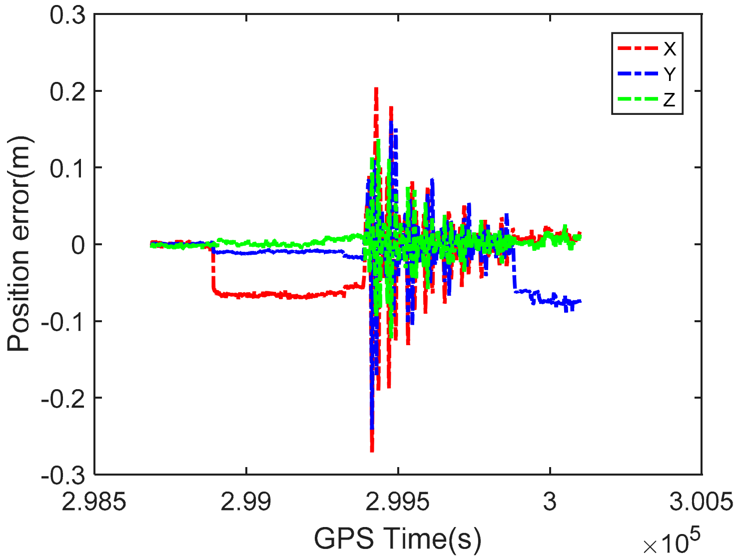

Figure 8. The position error of the tightly coupled system.

4.2. GNSS-Denied Environment

The experimental data were collected in Calgary, Canada. In the experiment, the GNSS data of the reference station and rover station with 1 Hz were collected by a NovAtel dual-frequency receiver. The reference station was located on the roof of the building, and the coordinates were expressed by geodetic coordinates (51.1163604880°, −114.0383357250°, 1044.751 m). The IMU raw data was collected using NovAtel's SPAN-FSAS, and the data sampling rate was 200 Hz. The specific technical parameters are shown in Table 3. The data collection time was about 28 min, and the maximum baseline length was about 8.5 km. In the experiment, dual-frequency data of the GPS was used for analysis, and the GPS/INS dual-frequency carrier tightly coupled smoothed result solved by the commercial software IE8.8 was used as a reference value.

Table 3. The technical parameters of SPAN-FSAS.

IMU	Bias	Random Walk	Scale Factor
Gyroscopes	0.75 deg/h	0.16 deg/sqrt (h)	300 ppm
Accelerometers	1.0 mg	50 ug/sqrt (Hz)	300 ppm

Figure 9 shows the number of satellites visible in the experiment and the PDOP value of the rover. It can be seen from the figure that the visible number of satellites in the first third of the experiment was about nine, and the observation environment was good. This was because the IMU was aligning and waiting for some time after alignment to obtain enough observation satellites and make the receiver converge faster. In the middle part of the experiment, because there were many trees and viaducts in the observation environment and the distance between the viaducts was relatively close, the number of visible satellites began to decrease and change frequently, from 6–9 to 2–4. In the last part of the experiment, the number of visible satellites was very small, basically within five, and there were more than two satellites in the period. The main reason for this is that the signal is almost completely interrupted when entering dense urban buildings, and the GPS positioning results will therefore become particularly poor or even unable to be used for positioning. The PDOP value of the rover further reflects the poor satellite geometry. Figure 10 shows the velocity of the vehicle during the experiment. In the first third of the experiment, the velocity of the vehicle was zero, which further verifies the analysis in Figure 9.

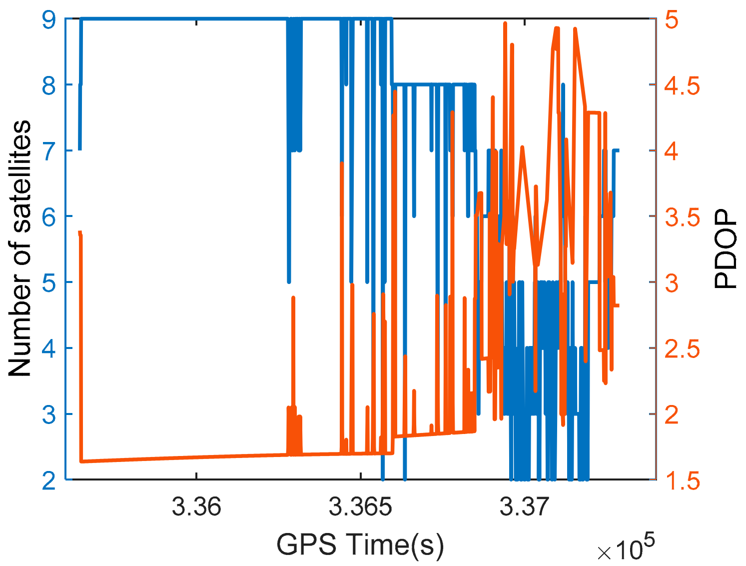

Figure 9. The number of visible satellites and the PDOP.

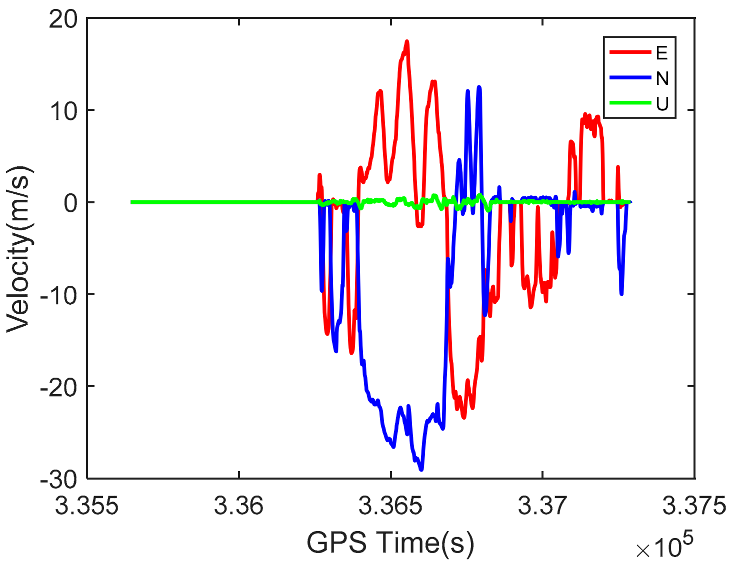

Figure 10. The velocity of the reference trajectory.

Figure 11 shows the trajectory of the GPS solution and the tightly coupled solution with the reference value. It can be seen from the figure that, in the first half of the experiment, the results of the GPS solution and the tightly coupled solution were consistent with the reference trajectory, and there was no obvious deviation. However, in the second half of the experiment, especially when entering the dense urban buildings, the GPS solution obviously deviated and took a long time, while the trajectory of the tightly coupled solution slightly deviated but was consistent with the reference trajectory, which indicates that INS can improve GPS continuity in a short time.

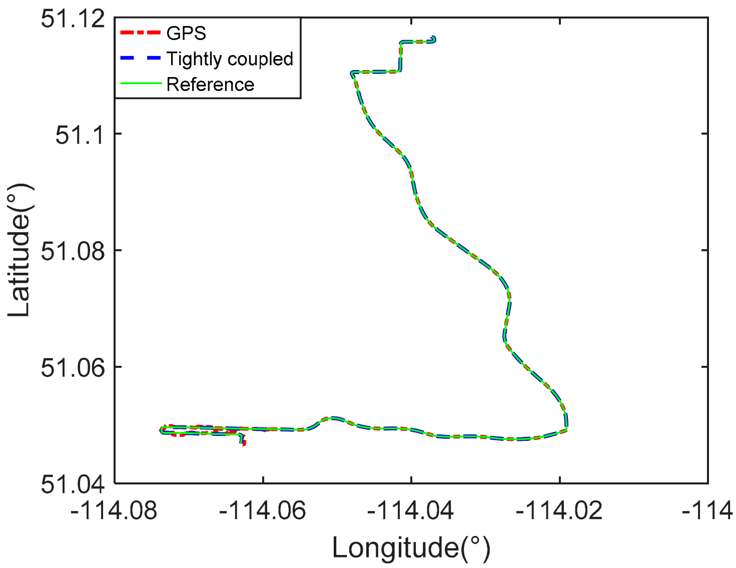

Figure 11. The trajectories of the three results.

For further analysis, their heights with reference values are given in Figure 12. Compared with the reference value, the highest height error of GPS was more than 300 m in dense buildings. In the beginning, the height of the tightly coupled system was consistent with the reference value at the dense place with buildings. However, it gradually deviated from the reference value with longer time of signal losing lock, and the maximum error reached more than 40 m. Figure 13 shows the ambiguity status of the GPS and the tightly coupled system. Compared with the GPS, the fixed ambiguity was slightly better than that of the GPS, and the fixed rates of ambiguity were 73% and 78.57% respectively.

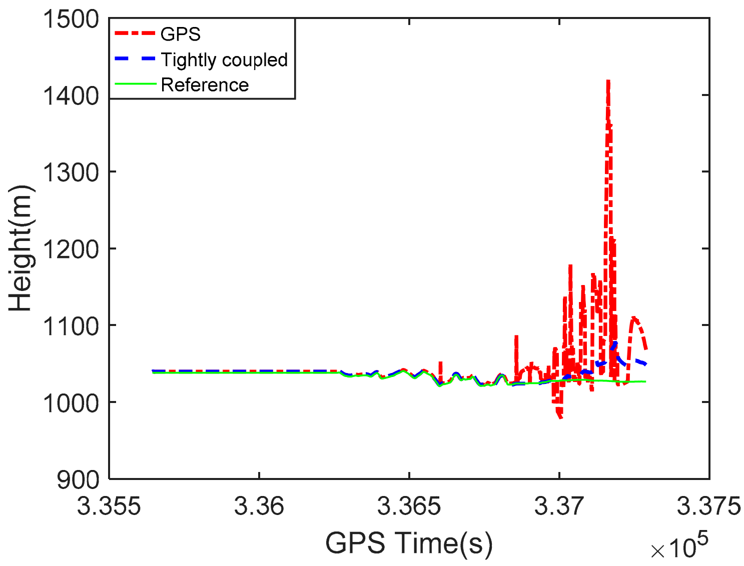

Figure 12. The height of the three results.

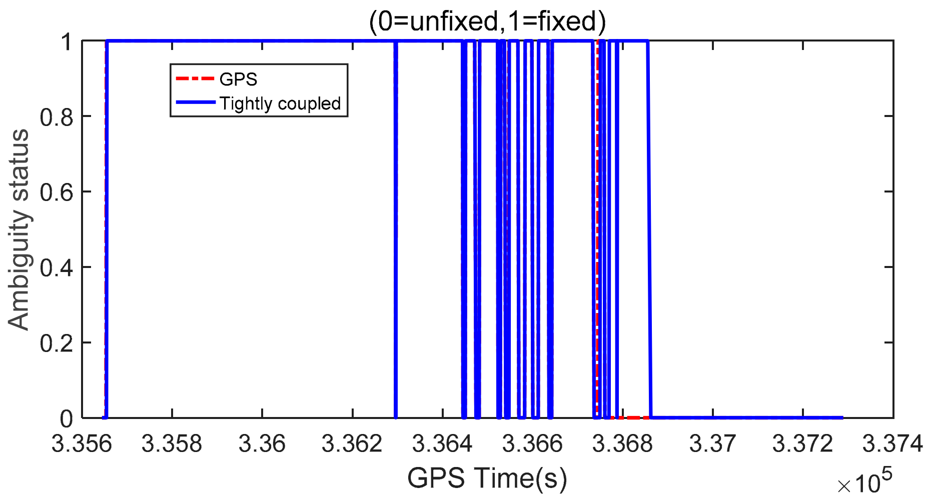

Figure 13. The ambiguity status of GPS and the tightly coupled system.

Figures 14 and 15 show the position errors of GPS and the tightly coupled system, respectively. The positioning accuracy of GPS was poor on the whole, and the error was especially large in the dense city, which made the overall error larger. For quantitative analysis, the statistical results of GPS and tightly coupled position errors are given in Table 4. It can be seen that the positioning errors of GPS were relatively large in all directions, being more than 15 m and as high as 33.220 m in the Z direction. Compared with GPS, the positioning errors of the tightly coupled system were lower, all being within 7 m and as low as 2.869 m in the X direction. Therefore, the tightly coupled system can effectively improve the positioning accuracy of GPS in a GNSS-denied environment.

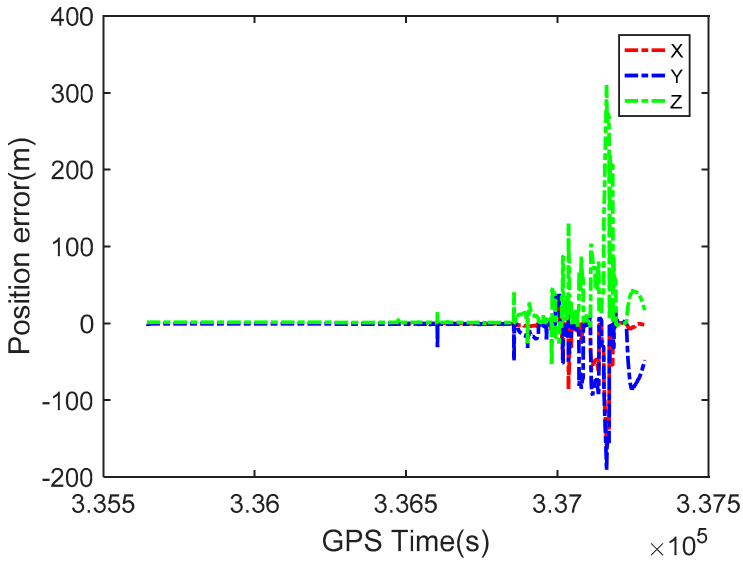

Figure 14. The position error of GPS.

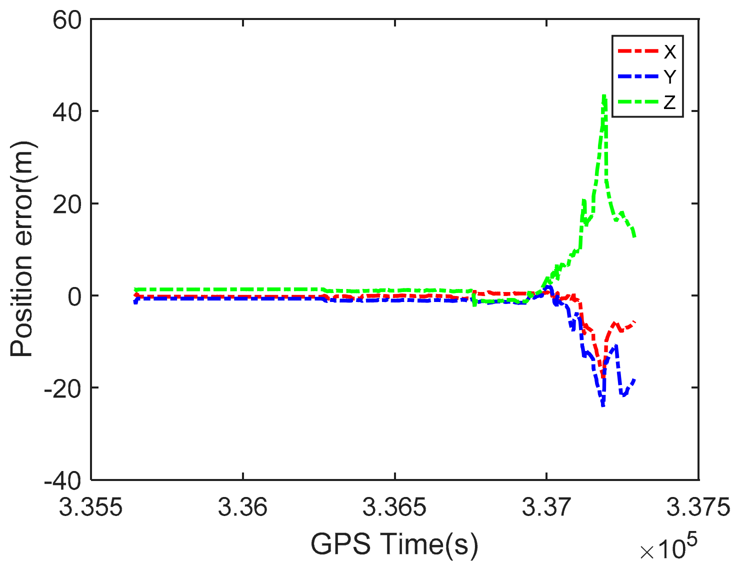

Figure 15. The position error of the tightly coupled system.

Table 4. The statistical results of position errors of GPS and the tightly coupled system.

		Maximum (m)	Minimum (m)	RMS (m)
GPS	X	26.777	−164.141	16.355
	Y	39.443	−190.476	23.795
	Z	309.926	−24.094	33.220
Tightly coupled system	X	1.144	−18.543	2.869
	Y	2.109	−24.094	5.028
	Z	43.608	−54.941	6.755

5. Discussion

The algorithm was evaluated by conducting two experiments, as shown in Section 4. In Experiment 1, in the open sky environment, many satellites could be seen, and the positioning accuracy of the tightly coupled system was the same as that of GPS, with no obvious difference. However, the ambiguity fixed rate of the tightly coupled system was slightly improved, all of them being above 97%. From another perspective, when the observation environment is good, GNSS can fully meet the needs of users, and the use of INS will also increase the cost. In Experiment 2, under a GNSS-denied environment, there were trees, viaducts, and dense urban buildings in the experimental environment. The number of visible satellites changed greatly, which led to poor quality of observation values. In the whole experiment, the positioning accuracy and continuity of the tightly coupled system were better than GPS. In the environment with trees and viaducts, the positioning accuracy of the tightly coupled system was slightly improved compared with GPS, which was mainly due to the high positioning accuracy of INS in a short time. When entering an urban dense building environment, the GPS signal is blocked or even interrupted, resulting in poor signal quality. At this time, the GPS ambiguity cannot be fixed, and it is the same for the tightly coupled system. However, in our experiment, the positioning accuracy of the tightly coupled system was significantly better than that of the GPS. The main reason for this is that, in addition to the high accuracy of INS in a short time, the algorithm proposed in this paper also made a contribution. The use of a wide-lane combination makes it easier to fix the ambiguity. The ambiguity parameter is added to the GNSS/INS state equation, which provides a higher accuracy float solution when the ambiguity cannot be fixed correctly. In addition, the residual test method also eliminates the outliers to some extent. However, the residual test here was mainly to test a single epoch and therefore needs to be improved. The test of multiple epochs is relatively complex and prone to errors, especially in a GNSS-challenged environment. In conclusion, the proposed algorithm can be used to solve the ambiguity of GNSS/INS tightly coupled system and can effectively improve the positioning accuracy and continuity of GPS.

Unfortunately, this paper mainly took GPS as an example to evaluate the positioning performance of the algorithm in different environments under a short baseline. Medium and long baselines were not considered because of the impact of the environment and difficulty in data collection. However, we are also making efforts to prepare for work on medium and long baseline data collection and hope to make a comprehensive evaluation of the algorithm and constantly improve it.

6. Conclusions

In this paper, a novel ambiguity parameter estimation and elimination strategy is proposed for GNSS/INS tightly coupled integration. Here, the ambiguity parameter in the carrier phase is added to the filter state equation for estimation. At the same time, to improve the ambiguity fixed success rate, the observation model of a single-frequency and wide-lane combination is used. To avoid too many parameters in the state equation, thereby resulting in a large calculation workload, the strategy of eliminating parameters is adopted, that is, when the ambiguity parameters are fixed and no cycle slip occurs, the ambiguity parameters are removed from the state equation and no longer estimated, which can reduce the complexity of the filter. However, during the filtering estimation process of the above strategy, if a satellite's ambiguity estimation has deviated, it can easily affect the entire filtering process. Therefore, a residual test strategy is used. After each epoch is estimated, the outliers or estimation deviations are tested by a residual test to reduce or avoid the impact on the next epoch. To evaluate the performance of the above strategy in a GNSS/INS tightly coupled system, vehicle experiments were conducted in an open sky environment and a GNSS-denied environment. The results showed that, compared with the GNSS positioning results, the positioning accuracy of the tightly coupled system was improved, especially in the GNSS-denied environment. Compared with GNSS, the ambiguity success fixed rate was also improved. In general, the ambiguity estimation and elimination strategy proposed for the tightly coupled system can effectively improve positioning accuracy and continuity. Our future research will mainly focus on the ambiguity resolution of a multifrequency multisystem GNSS/INS tightly coupled system under a GNSS-challenged environment.

Author Contributions: Conceptualization, C.M. and Q.Z.; methodology, C.M. and Q.Z.; software, C.M. and Q.Z.; validation, C.M. and Q.Z.; formal analysis, Q.Z. and C.M.; investigation, C.M.; resources, N.Z.; data curation, Q.Z. and X.M.; writing—original draft preparation, C.M.; writing—review and editing, Q.Z. and S.P.; visualization, Q.Z. and C.M.; supervision, Q.Z.; project administration, Q.Z.; funding acquisition, Q.Z. All authors have read and agreed to the published version of the manuscript.

Funding: This research project was jointly supported by the National Key R & D Program of China (2017YFE0119600, 2016YFC0803101), the National Natural Science Foundation of China (No. 42074226), the Open Research Fund of Jiangsu Key Laboratory of Resources and Environmental Information Engineering (JS201904), and the Priority Academic Program Development of Jiangsu Higher Education Institutions (PAPD).

Acknowledgments: We thank all the mission scientists and principal investigators who prepared and provided the data used in this study.

Conflicts of Interest: The authors declare no conflict of interest.

References

1. Deng, C.; Tang, W.; Liu, J.; Shi, C. Reliable single-epoch ambiguity resolution for short baselines using combined GPS/BeiDou system. *GPS Solut.* **2014**, *18*, 375–386. [CrossRef]
2. Odolinski, R.; Teunissen, P.J.; Odijk, D. Combined BDS, Galileo, QZSS and GPS single-frequency RTK. *GPS Solut.* **2013**, *19*, 151–163. [CrossRef]
3. Godha, S.; Cannon, M.E. GPS/MEMS INS integrated system for navigation in urban areas. *GPS Solut.* **2007**, *11*, 193–203. [CrossRef]
4. Ding, W.; Wang, J.; Rizos, C.; Kinlyside, D. Improving Adaptive Kalman Estimation in GPS/INS Integration. *J. Navig.* **2007**, *60*, 517–529. [CrossRef]
5. Zhang, Q.; Meng, X.; Zhang, S.; Wang, Y. Singular value decomposition-based robust cubature Kalman filtering for an integrated GPS/SINS navigation system. *J. Navig.* **2015**, *68*, 549–562. [CrossRef]
6. Grejnerbrzezinska, D.A.; Da, R.; Toth, C.K. GPS error modeling and OTF ambiguity resolution for high-accuracy GPS/INS integrated system. *J. Geod.* **1998**, *72*, 626–638. [CrossRef]
7. Li, Z.; Gao, J.; Wang, J. Inertial Aided Cycle Slip Detection and Repair for PPP/INS Tightly Coupled Navigation. *J. Navig.* **2016**, *69*, 1357–1378. [CrossRef]
8. Li, Q.; Ai, L.; Xiao, J.; Hsu, L.; Kamijo, S.; Gu, Y. Tightly coupled RTK/MIMU using single frequency BDS/GPS/QZSS receiver for automatic driving vehicle. In Proceedings of the IEEE/ION position, location and navigation symposium (PLANS), Monterey, CA, USA, 23–26 April 2018.
9. Lan, H.Y.; Elsheikh, M.; Abdelfatah, W.; Wahdan, A.; Naser, S. Integrated RTK/INS Navigation for Precision Agriculture. In Proceedings of the 32nd International Technical Meeting of the Satellite Division of The Institute of Navigation, Miami, FL, USA, 16–20 September 2019.
10. Falco, G.; Pini, M.; Marucco, G. Loose and Tight GNSS/INS Integrations: Comparison of Performance Assessed in Real Urban Scenarios. *Sensors* **2017**, *17*, 255. [CrossRef]
11. Chen, C.; Chang, G. Low-cost GNSS/INS integration for enhanced land vehicle performance. *Meas. Sci. Technol.* **2020**, *31*, 1–10. [CrossRef]
12. Yu, H.; Han, H.; Wang, J.; Xiao, H.; Wang, C. Single-Frequency GPS/BDS RTK and INS Ambiguity Resolution and Positioning Performance Enhanced with Positional Polynomial Fitting Constraint. *Remote Sens.* **2020**, *12*, 2374. [CrossRef]
13. Teunissen, P.J.G. The least-squares ambiguity decorrelation adjustment: A method for fast GPS integer ambiguity estimation. *J. Geod.* **1995**, *70*, 65–82. [CrossRef]
14. Teunissen, P.J.G. An optimality property of the integer least-squares estimator. *J. Geod.* **1999**, *73*, 587–593. [CrossRef]
15. Wu, H. On-the-fly GPS ambiguity resolution with inertial aiding. Ph.D. Thesis, The University of Calgary, Calgary, AB, Canada, 20 July 2003.
16. Skaloud, J. Reducing the GPS Ambiguity Search Space by Including Inertial Data. In Proceedings of the International Technical Meeting of ION, Nasgville, TN, USA, 15–18 September 1998.
17. Chen, A.; Zheng, D.; Ramanandan, A.; Farrell, J.A. INS aided GPS integer ambiguity resolution. In Proceedings of the IEEE International Conference on Control Applications (CCA), Denver, CO, USA, 28–30 September 2011.
18. Lee, H.K.; Wang, J.; Rizos, C. An integer ambiguity resolution procedure for GPS/pseudolite/INS integration. *J. Geod.* **2005**, *79*, 242–255. [CrossRef]

19. Gan, Y.; Sui, L.; Dong, M.; Liu, Q.; Chen, Q. INS aided direct calculation algorithm for single-epoch ambiguity resolution. *Geomat. Inf. Sci. Wuhan Univ.* **2016**, *41*, 1379–1384.
20. Han, H.; Wang, Q.; Wang, J. Robust ambiguity resolution for single-frequency GPS/BDS/MEMS IMU tightly coupled system. *J. Chin. Inert. Technol.* **2015**, *23*, 493-49.
21. Han, H.; Wang, J.; Wang, J.; Moraleda, A.H. Reliable partial ambiguity resolution for single-frequency GPS/BDS and INS integration. *GPS Solut.* **2017**, *21*, 251–264. [CrossRef]
22. Li, T.; Zhang, H.; Gao, Z.; Chen, Q.; Niu, X. High-Accuracy Positioning in Urban Environments Using Single-Frequency Multi-GNSS RTK/MEMS-IMU Integration. *Remote Sens.* **2018**, *10*, 205. [CrossRef]
23. Li, W.; Li, W.; Cui, X.; Zhao, S.; Lu, M. A Tightly Coupled RTK/INS Algorithm with Ambiguity Resolution in the Position Domain for Ground Vehicles in Harsh Urban Environments. *Sensors* **2018**, *18*, 2160. [CrossRef]
24. Li, T.; Zhang, H.; Gao, Z.; Niu, X.; El-sheimy, N. Tight Fusion of a Monocular Camera, MEMS-IMU, and Single-Frequency Multi-GNSS RTK for Precise Navigation in GNSS-Challenged Environments. *Remote Sens.* **2019**, *11*, 610. [CrossRef]
25. Liu, F.; Han, H.; Cheng, X.; Li, B. Performance of Tightly Coupled Integration of GPS/BDS/MEMSINS/Odometer for Real-Time High-Precision Vehicle Positioning in Urban Degraded and Denied Environment. *J. Sens.* **2020**, *4*, 1–15.
26. Qian, C.; Liu, H.; Tang, J.; Chen, Y.; Kaartinen, H.; Kukko, A.; Zhu, L.; Liang, X.; Chen, L.; Hyyppä, J. An Integrated GNSS/INS/LiDAR-SLAM Positioning Method for Highly Accurate Forest Stem Mapping. *Remote Sens.* **2017**, *9*, 3. [CrossRef]
27. Liu, S.; Sun, F.; Zhang, L.; Li, W.; Zhu, X. Tight integration of ambiguity-fixed PPP and INS: Model description and initial results. *GPS Solut.* **2016**, *20*, 39–49. [CrossRef]
28. Gao, Z.; Zhang, H.; Ge, M.; Niu, X.; Shen, W.; Wickert, J.; Schuh, H. Tightly coupled integration of multi-GNSS PPP and MEMS inertial measurement unit data. *GPS Solut.* **2017**, *21*, 377–391. [CrossRef]
29. Zhang, X.; Zhu, F.; Zhang, Y.; Mohamed, F.; Zhou, W. The improvement in integer ambiguity resolution with INS aiding for kinematic precise point positioning. *J. Geod.* **2019**, *93*, 993–1010. [CrossRef]
30. Gao, Z.; Ge, M.; Li, Y.; Pan, Y.; Chen, Q.; Zhang, H. Modeling of multi-sensor tightly aided BDS triple-frequency precise point positioning and initial assessments. *Inf. Fusion* **2020**, *55*, 184–198. [CrossRef]
31. Dorn, M.; Filwarny, J.O.; Wieser, M. Inertially-aided RTK based on tightly-coupled integration using low-cost GNSS receivers. In Proceedings of the European Navigation Conference (ENC), Lausanne, Switzerland, 9–12 May 2017.
32. Shin, E.H. *Estimation Techniques for Low-Cost Inertial Navigation*; University of Calgary: Calgary, AB, Canada, 2005.
33. Groves, P.D. *Principles of GNSS, Inertial, and Multisensor Integrated Navigation Systems*; Artech House: Norwood, MA, USA, 2013.
34. Jr, D.B.C.; Brading, J.D.W. Integration of LAMBDA Ambiguity Resolution with Kalman Filter for Relative Navigation of Spacecraft. *Navigation* **2000**, *47*, 205–210.
35. Teunissen, P.J.G.; Salzmann, M.A. A recursive slippage test for use in state-space filtering. *Manuscr. Geod.* **1989**, *14*, 383–390.
36. Teunissen, P.J.G. Quality control in integrated navigation systems. *IEEE Aerosp. Electron. Syst. Mag.* **1990**, *7*, 35–41. [CrossRef]